# Multipolar interactions in the D pocket of thrombin: large differences between tricyclic imide and lactam inhibitors†

**Eliane Schweizer,[a] Anja Hoffmann-Röder,[b] Jacob A. Olsen,[a] Paul Seiler,[a] Ulrike Obst-Sander,[c] Björn Wagner,[c] Manfred Kansy,[c] David W. Banner*[c] and François Diederich*[a]**

***Received 21st February 2006, Accepted 12th April 2006***
***First published as an Advance Article on the web 10th May 2006***
**DOI: 10.1039/b602585d**

Two series of tricyclic inhibitors of the serine protease thrombin, imides (±)-**1**–(±)-**8** and lactams (±)-**9**–(±)-**13**, were analysed to evaluate contributions of orthogonal multipolar interactions with the backbone C=O moiety of Asn98 to the free enthalpy of protein–ligand complexation. The lactam derivatives are much more potent and more selective inhibitors ($K_i$ values between 0.065 and 0.005 μM, selectivity for thrombin over trypsin between 361- and 1609-fold) than the imide compounds ($K_i$ values between 0.057 and 23.7 μM, selectivity for thrombin over trypsin between 3- and 67-fold). The increase in potency and selectivity is explained by the favorable occupancy of the P-pocket of thrombin by the additional isopropyl substituent in the lactam derivatives. The nature of the substituent on the benzyl ring filling the D pocket strongly influences binding potency in the imide series, with $K_i$ values increasing in the sequence: F < $OCH_2O$ < Cl < H < OMe < OH < $N_{pyr}$ ≪ Br. This sequence can be explained by both steric fit and the occurrence of orthogonal multipolar interactions with the backbone C=O moiety of Asn98. In contrast, the substituent on the benzyl ring hardly affects the ligand potency in the lactam series. This discrepancy was clarified by the comparison of X-ray structures solved for co-crystals of thrombin with imide and lactam ligands. Whereas the benzyl substituents in the imide inhibitors are sufficiently close (≤3.5 Å) to the C=O group of Asn98 to allow for attractive orthogonal multipolar interactions, the distances in the lactam series are too large (≥4 Å) for attractive dipolar contacts to be effective.

## Introduction

Over recent years, we have pursued the systematic substitution of H- for F-atoms ("fluorine scan") in nonpeptidic, tricyclic inhibitors[1] of thrombin in order to map the fluorophilicity/fluorophobicity of an entire enzyme active site.[2,3] During H/F substitution of the benzyl ring, which fills the hydrophobic distal (D) pocket (Fig. 1) of the serine protease from the blood coagulation cascade,[4] we had observed by X-ray analysis of a co-crystal a short orthogonal contact between the C–F residue of (±)-**1** and the backbone C=O of Asn98 ($d$(F···C=O) = 3.5 Å, angle $\alpha$(F···C=O) = 96°).[2a,b] Database mining subsequently revealed the frequent occurrence of similar electrostatic contacts both in small-molecule crystal structures (Cambridge Structural Database (CSD)) and in co-crystal structures of protein–ligand complexes (Protein Databank (PDB)). Therefore, we proposed that multipolar orthogonal C–F···C=O interactions are a significant contributor to the gain in binding free enthalpy ($\Delta\Delta G_{(\pm)\text{-}\mathbf{2}\rightarrow(\pm)\text{-}\mathbf{1}} = -4.4 \pm 0.7$ kJ mol$^{-1}$) measured upon changing from H-substituted (±)-**2** (inhibitory constant $K_i$ = 0.31 μM) to F-substituted (±)-**1** ($K_i$ = 0.057 μM). Subsequently, we quantified the attractive nature of orthogonal C–F···C=O interactions in model studies.[5] Furthermore, we documented in a comprehensive review the general occurrence of such orthogonal electrostatic interactions between dipoles in structural chemistry and biology.[6]

Here, we report the synthesis and biological activity of a series of new thrombin inhibitors, consisting of tricyclic imides (±)-**5**–(±)-**8** and tricyclic lactams (±)-**12** and (±)-**13**. Their inhibitory potencies and physicochemical properties (p$K_a$, log $D$) are compared to those of the previously described imides (±)-**1**–(±)-**4** and lactams (±)-**9**–(±)-**11**.[1,2a,b,16] By this comparison, we intended to explore how binding affinity changes when different dipoles such as C–F, C–Br, C–O and C=$N_{pyridyl}$ interact with the backbone C=O of Asn98 in the D pocket. The results of this study are quite surprising: whereas large differences in binding affinity are observed in the series of the tricyclic imide inhibitors, the substituted lactams are nearly equipotent. The structures of co-crystals of thrombin with the active (3a*S*,4*R*,8a*S*,8b*R*)-configured enantiomers of lactams (±)-**12** and (±)-**13** were solved, and X-ray structural comparisons finally provided an explanation for the unexpected differences in binding behaviour between the two classes of ligands.

## Results and discussion

### Synthesis of the tricyclic thrombin inhibitors

The synthesis of the new inhibitors followed earlier published protocols.[2b,7] The 1,3-dipolar cycloadditions between maleimides

[a]*Laboratorium für Organische Chemie, ETH-Zürich, Hönggerberg HCI, CH-8093, Zürich, Switzerland. E-mail: diederich@org.chem.ethz.ch; Fax: +41 44 6321109; Tel: +41 44 6322992*
[b]*Institut für Organische Chemie, Johannes Gutenberg-Universität, Duesbergweg 10-14, D-55128, Mainz, Germany*
[c]*Pharma Division, Präklinische Forschung, F. Hoffmann–La Roche AG, CH-4070, Basel, Switzerland*

† Electronic supplementary information (ESI) available: Synthesis of precursors to the new inhibitors, crystal packing and overlay of enzyme–ligand co-crystal structures. See DOI: 10.1039/b602585d

 

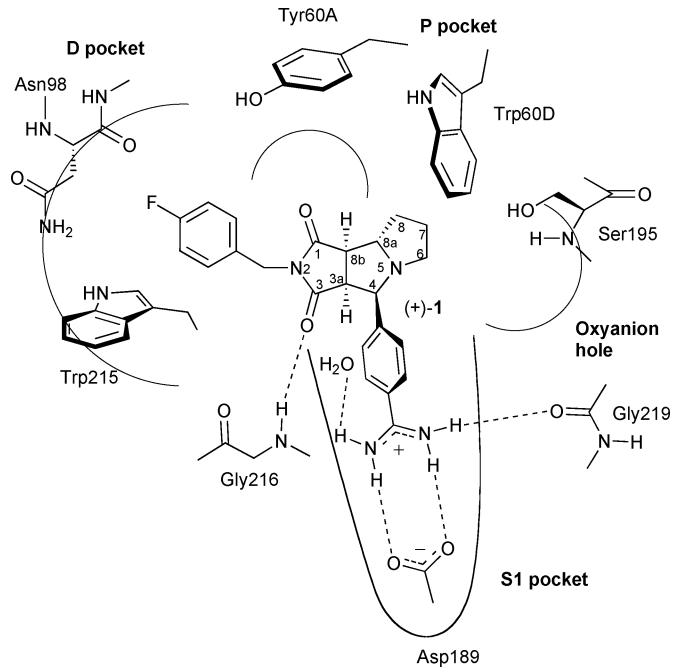


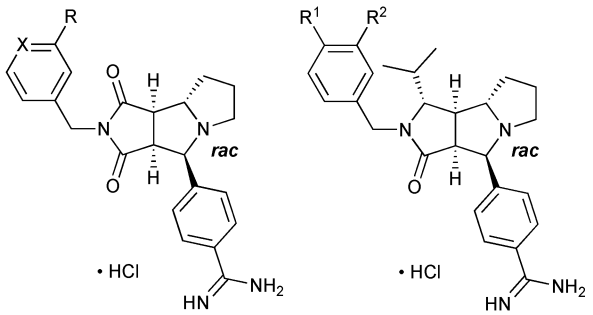


| | X | R |
|---|---|---|
| (±)-**1** | C–F | H |
| (±)-**2** | C–H | H |
| (±)-**3** | C–$OCH_2O$ | |
| (±)-**4** | C–Cl | H |
| (±)-**5** | C–Br | H |
| (±)-**6** | C–OMe | H |
| (±)-**7** | N | H |
| (±)-**8** | C–OH | H |

| | $R^1$ | $R^2$ |
|---|---|---|
| (±)-**9** | F | H |
| (±)-**10** | H | H |
| (±)-**11** | $OCH_2O$ | |
| (±)-**12** | Cl | H |
| (±)-**13** | OMe | H |

**Fig. 1** Left: Schematic representation of the binding mode of the tricyclic inhibitors in the active site of thrombin. The active site is defined by the catalytic centre with the nucleophilic Ser195 and the oxanion hole, the selectivity (S1) pocket, the large hydrophobic distal (D) pocket and a small proximal (P) pocket. Right: Inhibitors (±)-**1**–(±)-**8** and (±)-**9**–(±)-**13** investigated in this study. Only the (3a*S*,4*R*,8a*S*,8b*R*)-configured enantiomer is bound.[1,2]

**14**/**15**[8] (Scheme 1) and the azomethine ylide[9] formed from L-proline and 4-bromobenzaldehyde furnished in each case two of the possible four diastereoisomers ((±)-**16**/(±)-**18** starting from **14**, and (±)-**17**/(±)-**19** from **15**) which were separated chromatographically. Subsequent conversion of the desired *endo*,*trans*-configured diastereoisomers (see the caption to Scheme 1 for definitions) into nitriles (±)-**20**/(±)-**21** and Pinner reaction[10] afforded the tricyclic imide inhibitors (±)-**6** and (±)-**7**, respectively. Ether cleavage of (±)-**20** with $BBr_3$[11] to (±)-**22**, followed by the Pinner reaction, yielded ligand (±)-**8**. Ligand (±)-**5** was obtained by 1,3-dipolar cycloaddition between 4-bromobenzylmaleimide **23**[12] and the azomethine ylide formed from 4-formylbenzonitrile and L-proline, followed by separation of the diastereoisomeric cycloadducts (±)-**24**/(±)-**25** and Pinner reaction (Scheme 1).

The synthesis of the tricyclic lactam inhibitors (±)-**12** and (±)-**13**, directing an additional $Pr^i$ substituent into the P pocket of thrombin, also followed previously established protocols.[2b,7,16] Regio- and diastereoselective reduction of the 'upper' C=O group in (±)-**26** and (±)-**16**, using superhydride (Li[$Et_3BH$]) in THF, afforded the hydroxylactams (±)-**27** and (±)-**28**, respectively. We recently solved the X-ray crystal structure of the previously reported[2a,b] fluorinated hydroxylactam (±)-**29**, obtained by reduction of the corresponding imide under similar conditions. It shows that hydride attack occurred from the less hindered *exo*-side of the bicyclic perhydropyrrolo[3,4-*c*]pyrrole scaffold, leading to a *cis* orientation of the hydroxyl group with regard to the bromophenyl substituent (Fig. 2). We therefore assign to the newly created stereogenic centre in (±)-**27** and (±)-**28** the same configuration as seen for (±)-**29**. Similar diastereofacial selectivities in nucleophilic additions to *N*-benzylated tricyclic imide scaffolds, *e.g.* addition of $CF_3SiMe_3$,[13] have been observed before.

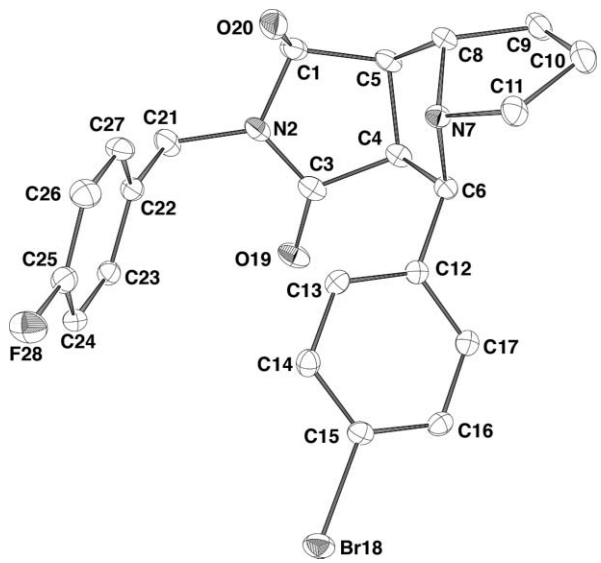


**Fig. 2** X-Ray crystal structure of the (C1*S*,C4*S*,C5*R*,C6*R*,C8*S*)-configured hydroxylactam **29**. Being a racemic mixture, an equal number of molecules with opposite stereochemistry are present in the crystal. Numbering is arbitrary. Atomic displacement parameters obtained at 173 K are drawn at the 30% probability level (for the crystal packing, see ESI).

The hydroxylactams (±)-**27** and (±)-**28** were converted into the corresponding sulfones (±)-**30** and (±)-**31**, respectively, upon reaction with *p*-toluenesulfinic acid in the presence of $CaCl_2$. Introduction of the desired isopropyl group in compounds (±)-**32** and (±)-**33** was achieved by displacement of the toluenesulfonyl group with $Pr^i MgCl$ in the presence of $ZnCl_2$.[14] In both steps, the nucleophile

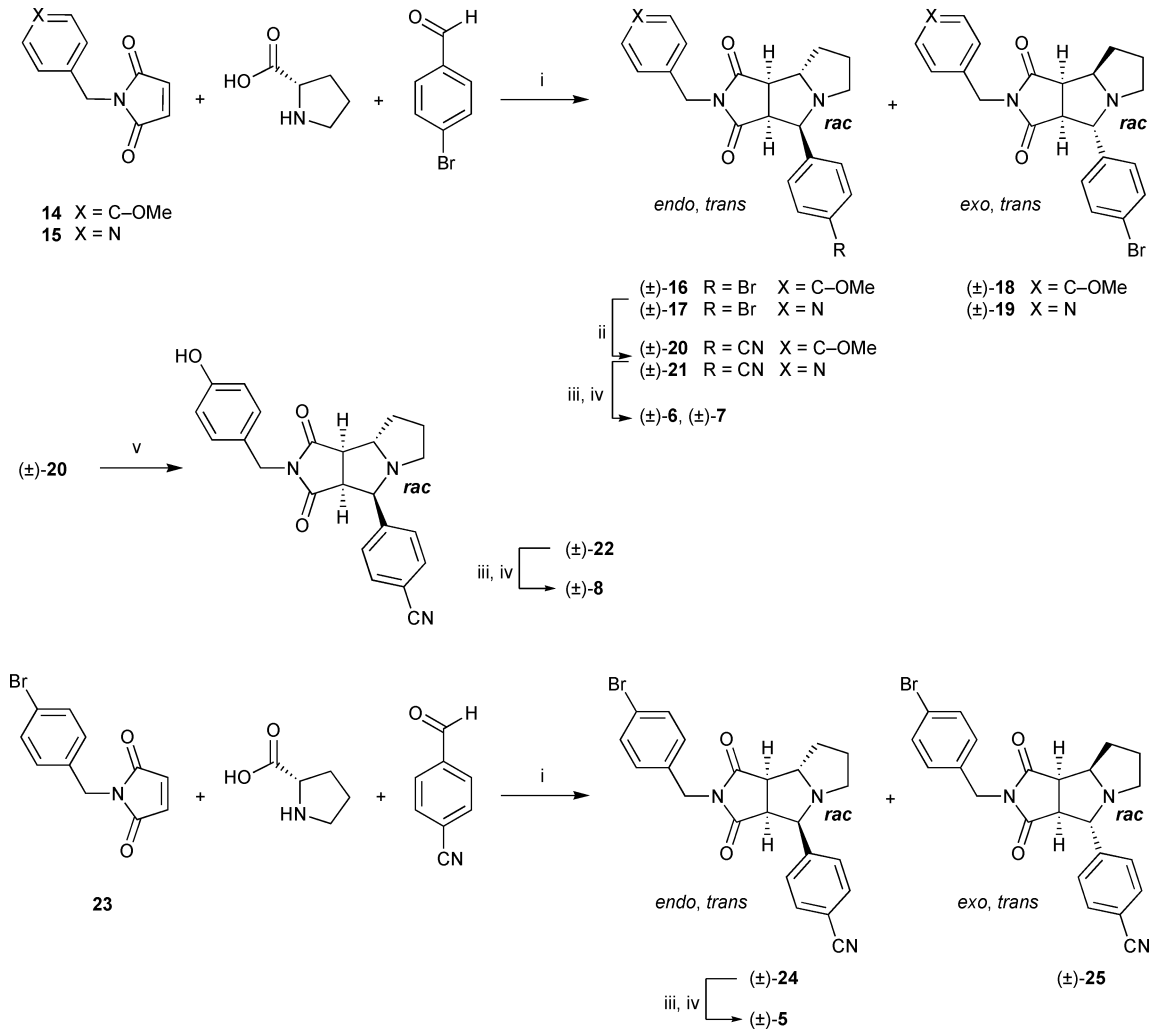


**Scheme 1** Synthesis of the tricyclic imide inhibitors. *Reagents and conditions*: (i) $CH_3CN$, 80 °C, 14–16 h; (±)-**16** (44%)/(±)-**18** (53%), (±)-**17** (35%)/(±)-**19** (18%), (±)-**24** (41%)/(±)-**25** (38%); (ii) CuCN, DMF, 165 °C, 24 h, or $[Pd_2(dba)_3]$ dppf, $Zn(CN)_2$, DMF, 120 °C, 24 h; (±)-**20** (78%), (±)-**21** (32%); (iii) MeOH, HCl(g), $CH_2Cl_2$, 4 °C, 28–35 h; (iv) $NH_3$, MeOH, 65 °C, 3 h; (±)-**5** (49%), (±)-**6** (21%), (±)-**7** (28%), (±)-**8** (40% from (±)-**20**); (v) $BBr_3$, $CH_2Cl_2$, −50 °C → 25 °C, 8 h. DMF = dimethylformamide, dba = dibenzylideneacetone, dppf = diphenylphosphinoferrocene. *Exo* and *endo* refer to the orientation of the 4-bromophenyl substituent at C(4) with respect to the bicyclic perhydropyrrolo[3,4-*c*]pyrrole scaffold, and *cis* and *trans* to the position of this 4-bromophenyl ring with respect to the configuration of C(8a) at the fusion of the two pentagons in the perhydropyrrolizidine bicycle (for atom numbering, see Fig. 1).

adds to the presumed acyliminium ion intermediate from the *exo* face of the bicyclic perhydropyrrolo[3,4-*c*]pyrrole scaffold. The targeted ligands (±)-**12** and (±)-**13** were finally obtained *via* nitriles (±)-**34** and (±)-**35**, again using the Pinner reaction (Scheme 2).

## Biological results

All newly prepared compounds were subjected to biological assays[15] to determine the inhibition constants for thrombin ($K_i$/μM) and the selectivity for thrombin over the digestive serine protease trypsin ($K_i$[Try]/$K_i$[Thr]). Furthermore, physicochemical properties (log *D* and p$K_a$) of the ligands were also determined following protocols previously described in great detail.[2c] Whereas the p$K_{a2}$ values of the phenylamidinium substituent are in the expected range (10.7 to 11.1), the p$K_{a1}$ values for the tertiary amine centres (4.4 to 4.6) in the tricyclic imides are remarkably low. As previously discussed,[2c] these low values are due to (i) the σ-inductive effect of the phenylamidinium ring in the α-position to the N-atom and (ii) the large σ-inductive effects of the two imide C=O moieties in the β-position. The latter explanation is nicely corroborated by the new results: upon changing from the imides (p$K_{a1}$ 4.4–4.6) to the lactams (p$K_{a1}$ 6.2–6.5), one of these σ-accepting pathways is removed and the acidity decreases substantially. The p$K_{a3}$ values of the pyridine and phenol substituents in (±)-**7** and (±)-**8** are in the expected range. The log *D* values (log *D* is the logarithmic coefficient of the distribution of a compound between octanol and water at pH 7.4) of all compounds (−0.4 to −1.6) are quite negative due to the phenylamidinium moiety.[2c] They expectedly increase slightly upon changing from the imide to the lactam inhibitors (*e.g.* compare the Cl-substituted imide (±)-**4** (log *D* −1.0) and lactam (±)-**12** (log *D* −0.4)). However, this increase in lipophilicity cannot explain the large differences in potency between imide- and lactam-based ligands, discussed below.

 

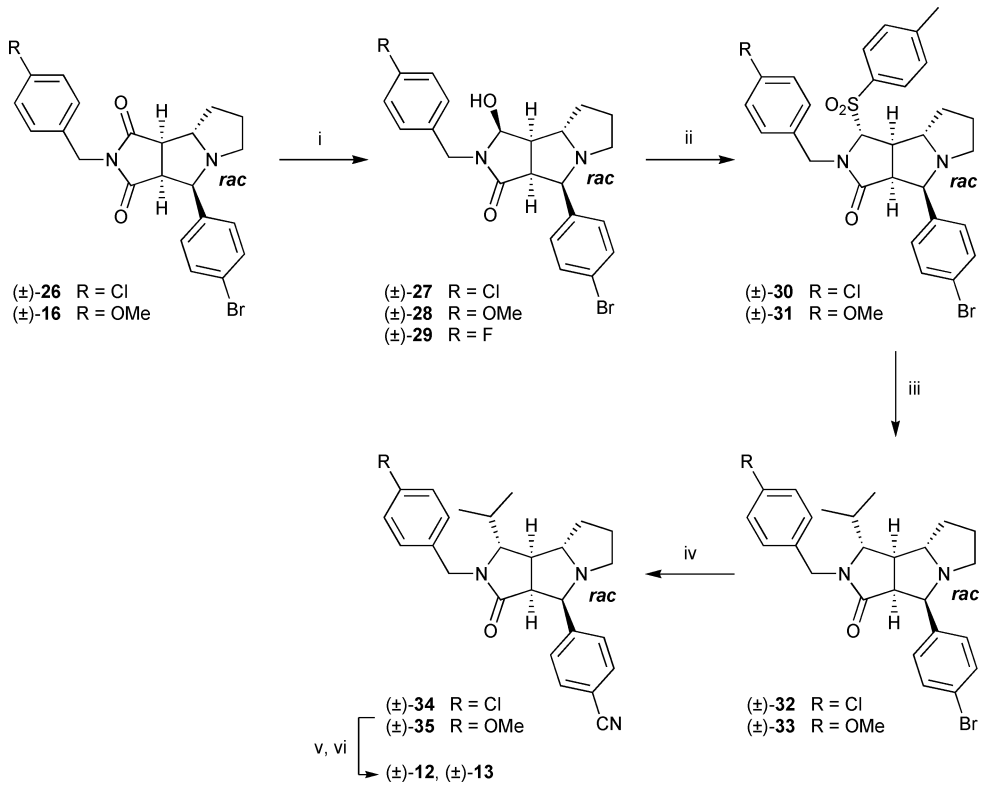


**Scheme 2** Synthesis of the tricyclic lactam inhibitors (±)-**12** and (±)-**13**. *Reagents and conditions*: (i) Li[$Et_3BH$], $CH_2Cl_2$, −78 °C → 0 °C, 2 h; (ii) 4-toluenesulfinic acid, $CaCl_2$, $CH_2Cl_2$, 25 °C, 5–7 d; (±)-**30** (32% from (±)-**26**), (±)-**31** (97% from (±)-**16**); (iii) $Pr^iMgCl$, $ZnCl_2$, $CH_2Cl_2$, 25 °C, 16–24 h; (±)-**32** (61%), (±)-**33** (46%); (iv) CuCN, DMF, 165 °C, 36 h or [$Pd_2(dba)_3$], dppf, $Zn(CN)_2$, DMF, 120 °C, 24 h; (±)-**34** (43%) (±)-**35** (62%); (v) MeOH, HCl(g), $CH_2Cl_2$, 4 °C, 28–35 h; (vi) $NH_3$, MeOH, 65 °C, 3 h; (±)-**12** (55%), (±)-**13** (25%).

The chromogenic binding assay confirmed that the lactam derivatives are both more potent and more selective thrombin inhibitors than the imide-based ligands. In the imide series, inhibitory strength varies between $K_i$ = 0.057 and 23.7 μM, whereas the lactam derivatives show $K_i$ values between 0.065 and 0.005 μM. The large extra binding free enthalpy of the lactam inhibitors is gained by occupancy of the tight lipophilic P pocket of thrombin by the $Pr^i$ substituent. Note that natural substrates of thrombin also prefer directing a valine side-chain into this pocket.[4] The selectivity for thrombin over trypsin is also dramatically increased upon introduction of the $Pr^i$ substituent: while $K_i$[Try]/$K_i$[Thr] in the imide series amounts to a moderate 3–67-fold, the selectivity in the lactam series is excellent and varies between 361–1609-fold. Again, this greatly enhanced selectivity originates from the favorable occupancy of the P pocket of thrombin by the $Pr^i$ substituent, since this pocket is absent in trypsin.[1,7] The extremely high, 1609-fold selectivity of the 4-chlorophenyl derivative (±)-**12** is by far the largest measured for all tricyclic inhibitors prepared so far.[1,2,16]

The inhibitory constants in the series of imide inhibitors (±)-**1**–(±)-**8** vary greatly. If the substituent on the benzyl ring in the D pocket – the only variable in the series – is considered, $K_i$/M increases in the sequence F < $OCH_2O$ < Cl < H < OMe < OH < $N_{pyr}$ ≪ Br (Table 1). An overlay of the crystal structures of the thrombin complexes with (±)-**1** (F),[2a] (±)-**3** ($OCH_2O$)[1a] and (+)-**36** ($OCH_2O$)[17] (Fig. 3) shows that the inhibitors adopt a nearly identical position in the active site of thrombin while the surrounding protein stucture, in particular the residues lining the D pocket,[18] *i.e.* the loop segment Glu97A–Leu99, as well as Tyr60A and Trp215, are geometrically highly conserved. While we are well aware that a variety of factors such as lipophilicity and solvation (as expressed by log *D*) and van der Waals interactions (such as with $C_\alpha$–H of Asn98) certainly influence the measured $K_i$ values, we propose that multipolar interactions with the C=O group of Asn98 together with steric effects make important contributions to the observed differences in potency. In the halide series, potency decreases in the sequence F ((±)-**1**) > Cl ((±)-**4**) ≫ Br ((±)-**5**). While the F- and Cl-substituted derivatives undergo efficient, nearly orthogonal multipolar interactions with the C=O group,[2a,b,6] making them better inhibitors than unsubstituted (±)-**2**, the Br substituent is clearly too bulky to fit. When the F-atom in the co-crystal structure of (±)-**1** (PDB-code: 1OYT) is replaced by a Br-atom, the latter and the carbonyl C-atom of Asn98 are at a repulsive van der Waals distance of 3.2 Å; relaxing the ligand in the computer modeling[19] induces a substantial shift of the tricyclic inhibitor away from Asn98. The potency of the piperonyl-substituted ligand (±)-**3**, similar to that of (±)-**1**, is more difficult to compare, since its upper O-atom undergoes additional H-bonding to the HO residue of Tyr60A.[1a] Nevertheless, the distance of the second O-atom to the C-atom of Asn98 ($d$ = 3.4 Å) suggests also a favorable contribution from multipolar interactions. Such interactions should also contribute to the binding affinity of the MeO- ((±)-**6**) and HO- ((±)-**8**) substituted ligands,[2d] although this favorable contribution is presumably compensated by unfavorable steric interactions of the MeO residue (modeling) in the complex of (±)-**6** and unfavorable desolvation of the HO group in the complex

**Table 1** Inhibitory activities and physicochemical properties of the tricyclic thrombin inhibitors

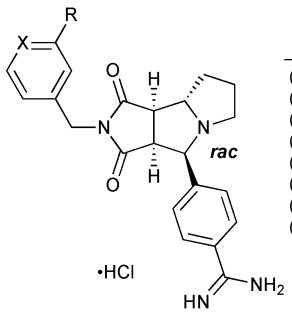


| | X | R |
|---|---|---|
| (±)-**1** | C–F | H |
| (±)-**2** | C–H | H |
| (±)-**3** | C–$OCH_2O$ | |
| (±)-**4** | C–Cl | H |
| (±)-**5** | C–Br | H |
| (±)-**6** | C–OMe | H |
| (±)-**7** | N | H |
| (±)-**8** | C–OH | H |

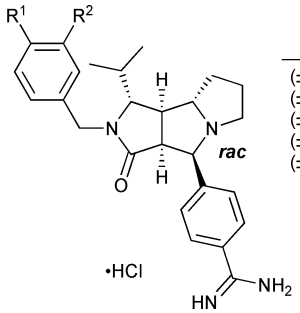


| | $R^1$ | $R^2$ |
|---|---|---|
| (±)-**9** | F | H |
| (±)-**10** | H | H |
| (±)-**11** | $OCH_2O$ | |
| (±)-**12** | Cl | H |
| (±)-**13** | OMe | H |

| | $K_i$/μM[a] | $K_i$[Try]/$K_i$[Thr] | p$K_{a1}$[b] | p$K_{a2}$[b] | p$K_{a3}$[b] | log $D$[c] |
|---|---|---|---|---|---|---|
| Imides: | | | | | | |
| (±)-**1**[d,e] | 0.057 | 67 | 4.47 | 11.14 | — | −1.16 |
| (±)-**2**[d,f] | 0.31 | 15 | n.d.[g] | n.d. | — | −0.99 |
| (±)-**3**[d,f] | 0.09 | 7.8 | n.d. | n.d. | — | n.d. |
| (±)-**4**[d,h] | 0.19 | 30 | 4.60 | 10.98 | — | −0.95 |
| (±)-**5**[d] | 23.7 | >2.9 | 4.56 | 11.11 | — | −0.69 |
| (±)-**6**[d] | 0.621 | 4.1 | 4.58 | 11.00 | — | −1.6 |
| (±)-**7**[d] | 1.54 | 15.4 | 4.38 | 10.97 | 3.75 | < −1 |
| (±)-**8**[d] | 0.89 | 9.7 | 4.62 | 10.72 | 9.32 | −1.22 |
| Lactams: | | | | | | |
| (±)-**9**[d,e] | 0.005 | 413 | 6.52 | n.d. | — | −0.81 |
| (±)-**10**[d,i] | 0.065 | 385 | n.d. | n.d. | — | −0.99 |
| (±)-**11**[d,j] | 0.013 | 760 | n.d. | n.d. | — | n.d. |
| (±)-**12**[d] | 0.008 | 1609 | 6.16 | n.d. | — | −0.37 |
| (±)-**13**[d] | 0.015 | 361 | 6.25 | 10.87 | — | −0.92 |

[a] The uncertainty of the measured $K_i$ values is ±20%. [b] p$K_{a1}$: tertiary amine in the tricyclic core; p$K_{a2}$: phenylamidinium; p$K_{a3}$: pyridine and phenol, respectively; accuracy of the p$K_a$ measurements: ± 0.1 p$K_a$ units. [c] Accuracy of the log $D$ measurements: ± 0.1 log $D$ units. [d] Only the (3a*S*,4*R*,8a*S*,8b*R*)-configured enantiomer is bound, as determined from the crystal structure analysis in refs. 1 and 2. [e] From ref. 2*a*. [f] From ref. 1*a*. [g] n.d. = not determined. [h] From ref. 2*b*. [i] From ref. 16. [j] From ref. 1*b*.

of (±)-**8**. The N-atom of the pyridine ligand is too far away (>3.9 Å) from the C=O group (modeling) to undergo any significant, strongly distance-dependent[6] multipolar interaction.

While the variation in potency is large in the series of tricyclic imide inhibitors, the four lactams (±)-**9**,[2a,b] (±)-**11**,[1b] (±)-**12** and (±)-**13** bearing substituents on the benzyl ring are nearly equipotent, with $K_i$ values varying between 0.005 and 0.015 μM. Since only one X-ray crystal structure of a lactam inhibitor ((±)-**11**) bound to thrombin existed prior to this work, the structures of the co-crystals formed by the new Cl- and MeO-substituted ligands were solved to 1.3 Å ((±)-**12**; PDB-code: 2CF8) and 1.79 Å ((±)-**13**; PDB-code: 2CF9) resolution. Fig. 4 depicts the chloro derivative (±)-**12** in the active site of thrombin, whereas the complex of the methoxy compound (±)-**13** is shown in Fig. 5. Both crystal structures clearly demonstrate that the electronegative O- and Cl-atoms attached to the 4-position of the benzyl residue in the tricyclic lactams are at much greater distance from the C=O group of Asn98 than in the protein-bound imide derivatives. In the complex of (±)-**12**, the distance $Cl \cdots C_{C=O(Asn)}$ amounts to 4.0 Å, and the same $O \cdots C$ distance is measured in the complex of (±)-**13**. At such large distances, multipolar interactions are no longer effective, which explains why the measured binding potencies are very similar. An overlay of crystal structures of imide and lactam inhibitors (ESI) provides another nice illustration of the different distances of the protein–ligand contacts seen in the D pocket.

## Conclusions

Two series of tricyclic inhibitors of the serine protease thrombin, imides (±)-**1**–(±)-**8** and lactams (±)-**9**–(±)-**13**, were analysed in order to evaluate the importance of orthogonal multipolar interactions in the hydrophobic D pocket of the enzyme. Physicochemical property analysis showed that the log $D$ values become less negative upon changing from the imide to the lactam series. Furthermore, the p$K_a$ value of the tertiary amine centre in the tricyclic scaffold increases by *ca.* 2 units when passing from the imide to the lactam ligands, mainly due to the removal of the σ-acceptor pathway between the N-atom and one β-C=O unit, thereby confirming earlier interpretations of the remarkably low p$K_a$ values (≈ 4.5) of this centre in the imide inhibitors.[2c] Biological assays demonstrated large differences between the potency of the imide and lactam series of inhibitors. In accordance with previous results, the lactam derivatives are much more potent and more selective inhibitors ($K_i$ values between 0.065 and 0.005 μM, selectivity for thrombin over trypsin between 361- and 1609-fold) than the imide compounds ($K_i$ values between 0.057 and 23.7 μM, selectivity for thrombin over trypsin between 3- and 67-fold). These differences originate from the favorable occupancy of the tight hydrophobic P pocket by the isopropyl residue of the lactam inhibitors; this pocket is absent in trypsin. In the imide series, binding potency is determined by the nature of the substituent on

 

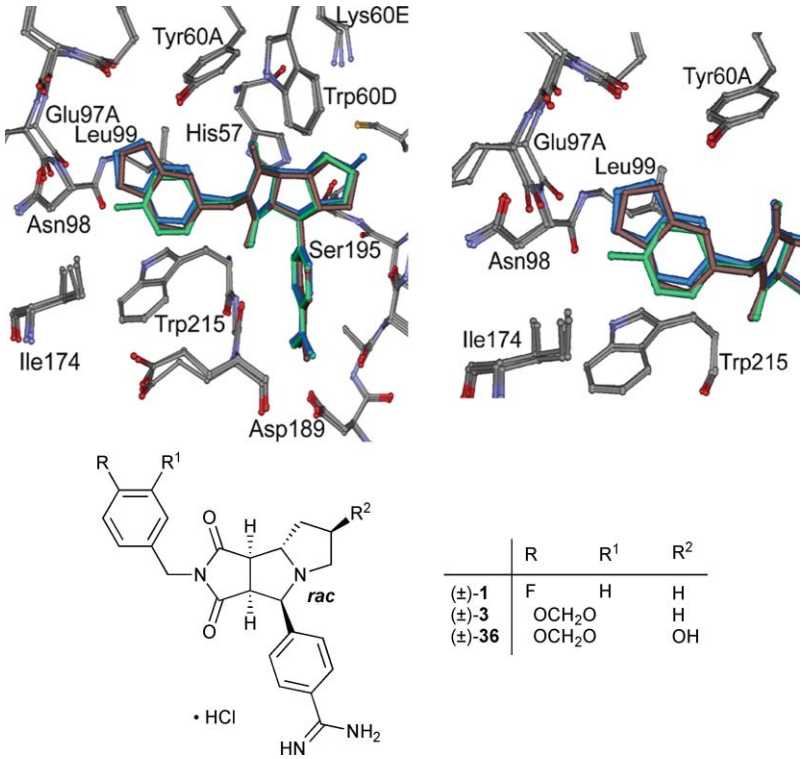


**Fig. 3** Left: Overlay of the co-crystal structures of the imide-based inhibitors (±)-**1** (PDB-Code: 1OYT),[2a] (±)-**36** (PDB-Code: 1VZQ)[17] and (±)-**3**[1a] with thrombin, as determined by X-ray crystallographic analysis, showing a nearly perfect superimposition of the protein residues and the inhibitors. Right: Zoom into the D pocket. Noticeable is the exact overlap of the backbone C=O group of Asn98, involved in multipolar interactions with the inhibitors. Color code: C-skeleton of (±)-**1**: green, (±)-**36**: blue, (±)-**3**: brown, C-skeleton of the protein: grey, O-atoms: red, N-atoms: blue, S-atoms: yellow.

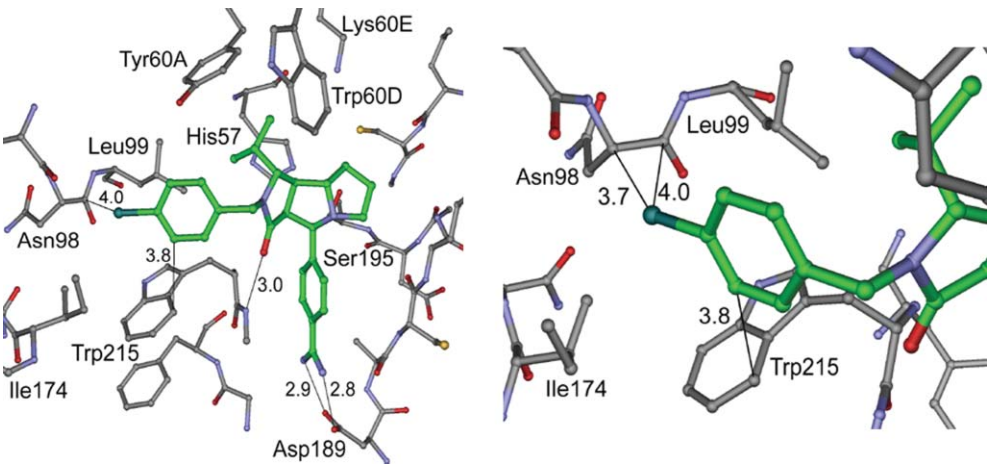


**Fig. 4** Left: Inhibitor (±)-**12** in the active site of thrombin as revealed by X-ray crystal structure analysis. Only the (3a*S*,4*R*,8a*S*,8b*R*)-configured enantiomer is bound. Right: Binding mode of the 4-chlorobenzyl moiety in the region of the D pocket of thrombin. Color code: C-skeleton of the inhibitor: green, C-skeleton of the protein: grey, O-atoms: red, N-atoms: blue, S-atoms: yellow, Cl-atom: dark green. Distances in Å.

the benzyl ring filling the D pocket, with $K_i$ values increasing in the sequence: F < $OCH_2O$ < Cl < H < OMe < OH < $N_{pyr}$ ≪ Br. This sequence can be explained by both steric fit and the occurrence of orthogonal multipolar interactions with the backbone C=O moiety of Asn98. In contrast, the substituent on the benzyl ring hardly affects the ligand potency in the lactam series. This discrepancy was clarified by solving two additional crystal structures of the Cl- and MeO-substituted lactams (±)-**12** and (±)-**13** bound to thrombin. Whereas the benzyl substituents in the imide inhibitors are sufficiently close (≤3.5 Å) to the C=O group of Asn98 to allow for efficient orthogonal multipolar interactions, the distances in the lactam series are too large (≥4 Å) for attractive dipolar contacts to occur. This study clearly shows that a large number of biological and structural data are required to map in detail the molecular recognition properties of a pocket in an enzyme active site, and to evaluate contributions of weak interactions such as multipolar contacts to the measured binding free enthalpies.

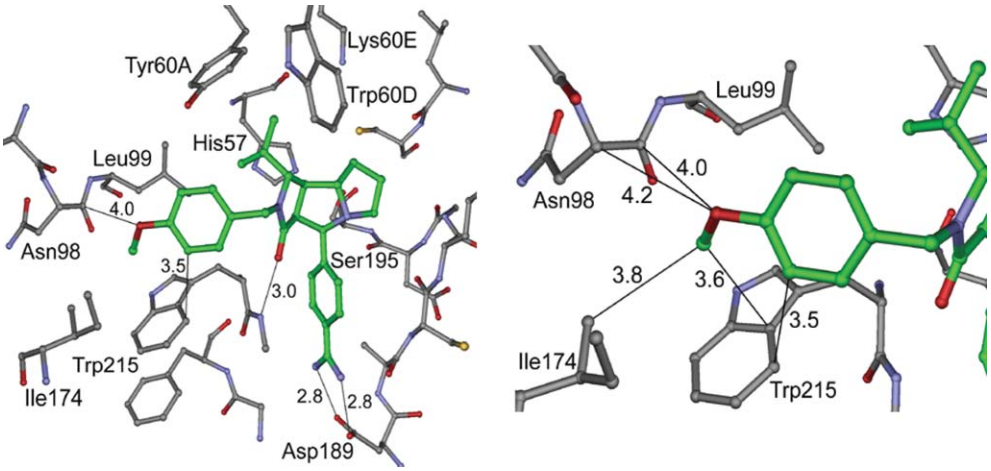


**Fig. 5** Left: Inhibitor (±)-**13** in the active site of thrombin as determined by X-ray crystallographic analysis. Only the (3a*S*,4*R*,8a*S*,8b*R*)-configured enantiomer is bound. Right: Binding mode of the 4-methoxybenzyl moiety in the D pocket of thrombin. Hydrophobic contacts between the methyl group and the protein are also shown. Color code: C-skeleton of the inhibitor: green, C-skeleton of the protein: grey, O-atoms: red, N-atoms: blue, S-atom: yellow. Distances in Å.

## Experimental

### General details

Solvents and reagents were reagent-grade, purchased from commercial suppliers, and used without further purification unless otherwise stated. 4-Toluenesulfinic acid was prepared according to a literature procedure.[20] The synthesis of (±)-**1**,[2b] (±)-**2**,[7] (±)-**3**,[7] (±)-**4**,[2b] (±)-**9**,[2b] (±)-**10**,[16] and (±)-**11**[7] followed published procedures. THF was freshly distilled from sodium benzophenone ketyl, and $CH_2Cl_2$ from $CaH_2$. HCl gas was dried with conc. $H_2SO_4$. If not mentioned otherwise, all products were dried under high vacuum ($10^{-2}$ Torr) before analytical characterisation. Column chromatography (CC) was conducted on silica gel 60 (230–400 mesh, 0.040–0.063 mm) from Fluka. Analytical thin layer chromatography (TLC) was conducted on silica gel 60-$F_{245}$ (on glass, Merck). Plates were visualised by UV light at 245 nm and staining with a solution of $KMnO_4$ (1.5 g), $K_2CO_3$ (10 g), 5% NaOH (2.5 $cm^3$) in $H_2O$ (150 $cm^3$); a solution of anisaldehyde (6.8 $cm^3$), conc. $H_2SO_4$ (9.2 $cm^3$) and acetic acid (2.8 $cm^3$) in EtOH (250 $cm^3$); or a solution of ninhydrin (0.3 g) in butanol (100 $cm^3$) and glacial acetic acid (3 $cm^3$). Melting points (mp) were determined using a Büchi-510 apparatus and are uncorrected. IR spectra were recorded on a Perkin–Elmer Spectrum BX FTIR System spectrometer (ATR-unit, Attenuated Total Reflection, Golden Gate). NMR spectra were recorded at 25 °C on Varian Gemini-300 and Bruker ARX-300 spectrometers. Chemical shifts $\delta$ are reported in ppm using the solvent peak as a reference. $J$ values are given in Hz. The exchangeable amidinium protons were not observed in $^1$H NMR spectra recorded in $CD_3OD$. High-resolution MALDI mass spectra (HR-MS) were recorded at IonSpec Ultima with 2,5-dihydroxybenzoic acid (DHB) as matrix, EI at *VG-TRIBRID*; molecular ions ($M^+$) reported for phenylamidinium salts refer to the corresponding phenylamidine derivatives. The nomenclature was generated with the computer programs AUTONOM (Beilstein) and ACD-Name (ACD/Labs). High-throughput log $D$ screening and p$K_a$ determinations by potentiometric titration were performed as previously described.[2c]

### Enzymatic assay for the determination of $K_i$

For the enzymatic assay, the release of *p*-nitroaniline by cleavage of the chromogenic substrate H–D-Phe–Pip–Arg-*p*-nitroanilide (S-2238)[15a] by means of thrombin was followed spectrophotometrically at 405 nm. The enzyme used for the assay was human thrombin prepared according to Fenton *et al.*[15b] The thrombin preparation contained 90% α-thrombin as determined by active-site titration and SDS-PAGE. For each measurement 30 µL of inhibitor and 20 µL of water were mixed with 180 µL of thrombin in buffer (2 nM fc; HEPES 100 mM, NaCl 140 mM, PEG 6000 0.1%, Tween 80 0.2%, pH 7.8) and incubated at 25 °C for 240 s. 50 µL of the substrate S-2238 (50 µM fc, $K_m$ 3.33 µM) and 20 µM of water were added, and the release of *p*-nitroaniline was recorded for 60 s at intervals of 10 s. Measurements were carried out at different inhibitor concentrations (in the range of 100–0.0001 µM in 1/10 dilution steps). The $K_i$ value was calculated [$K_i = IC_{50}/\{1 + (S/K_m)\}$] from the $IC_{50}$ value, determined graphically from the dose response curve of the inhibitor. An exhaustive protocol of the binding assay used in this study is provided in ref. 15*c*.

### General procedure A for the synthesis of *N*-alkylated maleimides

To a solution of maleic anhydride (182 mmol) in dry $CH_2Cl_2$ (300 $cm^3$) under Ar, 4-substituted benzylamine (182 mmol) was added over 30 min at 0 °C and the reaction stirred for 12 h at 25 °C. Under ice cooling, DMF (0.14 $cm^3$) and, over 2 h, oxalyl chloride (200 mmol) was added. The mixture was stirred for 24 h and the solvent evaporated. The residue was dried under high vacuum and dissolved in dry $CH_2Cl_2$ (200 $cm^3$) under Ar. $Et_3N$ (237 mmol) was added over 30 min, the mixture stirred at 25 °C for 2 h, and washed with 1 N HCl solution (3 × 150 $cm^3$). The org. phase was dried ($Na_2SO_4$), the solvent evaporated *in vacuo* and the residue purified by CC ($SiO_2$; cyclohexane–AcOEt 2 : 1).

### General procedure B for the 1,3-dipolar cycloaddition

A mixture of L-proline (24.2 mmol), 4-bromobenzaldehyde (24.2 mmol) or 4-formylbenzonitrile (24.2 mmol) and

 

*N*-substituted maleimide (24.2 mmol) in $CH_3CN$ (100 $cm^3$) was heated to 80 °C for 14–16 h. The solvent was evaporated *in vacuo* and the residue purified by CC ($SiO_2$; $CH_2Cl_2$–AcOEt 4 : 1 or 1 : 1).

**General procedure C for the reduction of an imide and conversion of the resulting hydroxylactam into a *p*-toluenesulfone**

To a solution of imide (7.2 mmol) in $CH_2Cl_2$ (50 $cm^3$) cooled to −78 °C, a solution of Li[$Et_3BH$] (19 mmol, 1 M in THF) was added. After 2 h, the mixture was warmed to 0 °C, sat. aq. $NaHCO_3$ (30 $cm^3$) was added, and the aqueous phase extracted with $CH_2Cl_2$ (100 $cm^3$). The organic layer was dried ($Na_2SO_4$) and evaporated *in vacuo.* The crude product, $CaCl_2$ (19.4 mmol) and 4-toluenesulfinic acid (19.4 mmol) were dissolved in $CH_2Cl_2$ (50 $cm^3$), and the mixture was stirred for 5–7 days. Sat. aq. $NaHCO_3$ (30 $cm^3$) was added and the aqueous phase extracted with $CH_2Cl_2$ (3 × 30 $cm^3$). The organic layer was dried ($Na_2SO_4$), evaporated *in vacuo* and the residue purified by CC ($SiO_2$; $CH_2Cl_2$–AcOEt 4 : 1) or recrystallized from AcOEt.

**General procedure D for the introduction of the isopropyl residue**

To a solution of $ZnCl_2$ (2.8 mmol, 1 M in $Et_2O$) in dry $CH_2Cl_2$ (30 $cm^3$), a solution of $Pr^iMgCl$ (5.2 mmol, 2 M in $Et_2O$) was added and the mixture stirred under Ar for 30 min. A solution of sulfone (2.6 mmol) in dry $CH_2Cl_2$ (50 $cm^3$) was slowly added under ice cooling and the mixture stirred for 16–24 h at 25 °C. After addition of 1 M HCl (20 $cm^3$), the mixture was neutralised with aq. $NaHCO_3$ (50 $cm^3$) and extracted with $CH_2Cl_2$ (3 × 80 $cm^3$). The organic phase was dried ($Na_2SO_4$), the solvent evaporated *in vacuo* and the residue purified by CC ($SiO_2$; cyclohexane–AcOEt 2 : 1 or $CH_2Cl_2$–AcOEt 1 : 2).

**General procedure E for the conversion of an aryl bromide into an aryl nitrile**

**Method A.** A well degassed suspension of CuCN (4.7 mmol) in dry DMF (5 $cm^3$) was heated to reflux under Ar for 30–60 min, before a degassed solution of bromide (1.2 mmol) in dry DMF (3 $cm^3$) was added and the mixture stirred for 24–36 h. The solvent was evaporated *in vacuo*, the residue dissolved in $CH_2Cl_2$ (10 $cm^3$) and conc. aq. $NH_4OH$ solution (5 $cm^3$) was added. The mixture was stirred at 25 °C for 1 h, the blue aqueous phase removed, the organic phase washed with conc. aq. $NH_4OH$ solution (10 $cm^3$) and sat. aq. NaCl solution (10 $cm^3$), dried ($Na_2SO_4$) and the solvent removed *in vacuo.* The residue was purified by CC ($SiO_2$; $CH_2Cl_2$–AcOEt 1 : 1).

**Method B.** To a suspension of [$Pd_2(dba)_3$] (0.04 mmol) and dppf (0.09 mmol) in degassed, dry DMF (3 $cm^3$) under Ar, a solution of bromide (0.7 mmol) in degassed, dry DMF (2 $cm^3$) and $Zn(CN)_2$ (0.7 mmol) were added. The mixture was stirred for 24 h at 120 °C, the solvent evaporated *in vacuo* and the residue purified by CC ($SiO_2$; cyclohexane–AcOEt 1 : 1).

**General procedure F for the preparation of amidinium salts (Pinner reaction)**

Dry HCl gas was bubbled at 0 °C for 10 min into a solution of the nitrile (0.5 mmol) in dry $CH_2Cl_2$ (0.6 $cm^3$) and dry MeOH (1.2 $cm^3$). The mixture was stored at 4 °C for 28–35 h, then the solvent was removed *in vacuo.* The residue was precipitated with $Et_2O$, filtrated and dried under high vacuum, then dissolved in a solution of $NH_3$ (2 $cm^3$, 7 M in MeOH) and stirred for 3 h at 65 °C. The solvent was evaporated *in vacuo* and the residue purified by CC ($SiO_2$; $CH_2Cl_2$–MeOH 9 : 1).

**4-(3a*SR*,4*RS*,8a*SR*,8b*RS*)- and 4-(3a*SR*,4*SR*,8a*RS*,8b*RS*)-(4-Bromophenyl)-2-(4-methoxybenzyl)hexahydropyrrolo[3,4-*a*]-pyrrolizin-1,3-dione ((±)-16 and (±)-18)**

General procedure B, starting from **14** (see ESI†) (5.00 g, 23.0 mmol), L-proline (2.79 g, 24.2 mmol) and 4-bromobenzaldehyde (4.47 g, 24.2 mmol) in $CH_3CN$ (100 $cm^3$), gave *endo*-adduct (±)-**16** (4.58 g, 44%) and *exo*-adduct (±)-**18** (5.55 g, 53%).

**Data for (±)-16.** Colorless solid; mp 137–139 °C; $\nu_{max}/cm^{-1}$ (neat) 3273, 2951, 2874, 1694, 1612, 1585, 1515, 1486, 1467, 1428, 1393, 1340, 1302, 1249, 1210, 1166, 1115, 1102, 1085, 1070, 1030; $\delta_H$(300 MHz; $CDCl_3$) 1.60–1.78 (2 H, m), 1.97–2.13 (2 H, m), 2.58–2.65 (1 H, m), 2.77–2.85 (1 H, m), 3.24 (1 H, d, *J* 8.1), 3.44 (1 H, t, *J* 8.4), 3.72–3.81 (1 H, m), 3.79 (3 H, s), 3.99 (1 H, d, *J* 8.7), 4.46 (2 H, s), 6.81, 7.06 (4 H, AA′BB′, *J* 8.6); 7.23, 7.34 (4 H, AA′BB′, *J* 8.7); $\delta_C$(75 MHz; $CDCl_3$) 23.4, 29.6, 41.9, 49.1, 50.4, 50.8, 55.3, 67.8, 68.2, 113.7, 121.4, 127.9, 129.6, 130.3, 131.1, 137.0, 159.1, 174.9, 177.7; MALDI-HR-MS calcd for $C_{23}H_{24}BrN_2O_3^+$ ([M + H]$^+$): 455.0965; found 455.0965.

**Data for (±)-18.** Colorless solid; mp 102–103 °C; $\nu_{max}/cm^{-1}$ (neat) 2934, 1772, 1702, 1611, 1586, 1512, 1483, 1424, 1393, 1336, 1305, 1292, 1239, 1167, 1110, 1099, 1037; $\delta_H$(300 MHz; $CDCl_3$) 1.49–1.60 (1 H, m), 1.63–1.72 (2 H, m), 1.89–1.95 (1 H, m), 2.36–2.44 (1 H, m), 2.87–2.95 (1 H, m), 3.25 (1 H, dd, *J* 9.0 and 5.8), 3.49 (1 H, t, *J* 9.0), 3.77 (3 H, s), 3.82–3.87 (1 H, m), 4.03 (1 H, d, *J* 5.6), 4.57 (2 H, s), 6.82, 7.34 (4 H, AA′BB′, *J* 8.7), 7.43, 7.45 (4 H, AA′BB′, *J* 8.7); $\delta_C$(75 MHz; $CDCl_3$) 24.4, 26.3, 42.0, 47.9, 52.0, 55.3, 55.5, 66.3, 69.0, 113.8, 121.1, 127.6, 128.5, 130.4, 131.5, 141.1, 159.2, 176.4, 177.5; MALDI-HR-MS calcd for $C_{23}H_{24}BrN_2O_3^+$ ([M + H]$^+$): 455.0965; found: 455.0964.

**4-(3a*SR*,4*RS*,8a*SR*,8b*RS*)- and 4-(3a*SR*,4*SR*,8a*RS*,8b*RS*)-(4-Bromophenyl)-2-pyridin-4-ylmethylhexahydropyrrolo[3,4-*a*]pyrrolizin-1,3-dione ((±)-17 and (±)-19)**

General procedure B, starting from **15** (see ESI†) (1.77 g, 9.4 mmol), L-proline (1.19 g, 10.3 mmol) and 4-bromobenzaldehyde (1.91 g, 10.3 mmol) in $CH_3CN$ (20 $cm^3$), gave *endo*-adduct (±)-**17** (1.41 g, 35%) and *exo*-adduct (±)-**19** (730 mg, 18%).

**Data for (±)-17.** Colorless solid; mp 69–72 °C; $\nu_{max}/cm^{-1}$ (neat) 2956, 2877, 1773, 1701, 1601, 1564, 1485, 1417, 1395, 1337, 1317, 1285, 1233, 1197, 1167, 1104, 1087, 1069, 1048, 1009; $\delta_H$(300 MHz; $CDCl_3$) 1.57–1.83 (2 H, m), 1.93–2.17 (2 H, m), 2.57–2.67 (1 H, m), 2.79–2.90 (1 H, m), 3.29 (1 H, d, *J* 8.1), 3.49 (1 H, dd, *J* 8.4 and 8.1), 3.70–3.77 (1 H, m), 4.02 (1 H, d, *J* 8.7), 4.49 (2 H, s), 7.07, 7.33 (4 H, AA′BB′, *J* 8.4), 7.13, 8.51 (4 H, AA′BB′, *J* = 5.9); $\delta_C$(75 MHz; $CDCl_3$) 23.5, 29.7, 41.4, 49.1, 50.7, 50.8, 68.1, 68.2, 121.8, 123.3, 129.8, 131.5, 136.9, 144.2, 150.3, 175.1, 177.9; MALDI-HR-MS calcd for $C_{21}H_{21}BrN_3O_2^+$ ([M + H]$^+$): 426.0812; found: 426.0803.

**Data for (±)-19.** Brown solid; mp 65–67 °C; $\nu_{max}/cm^{-1}$ (neat) 2966, 2879, 1773, 1698, 1601, 1485, 1416, 1393, 1338, 1314, 1241,

1165, 1069, 1009; $\delta_H$(300 MHz; $CDCl_3$) 1.42–1.55 (1 H, m), 1.67–1.77 (2 H, m), 1.87–1.99 (1 H, m), 2.40–2.49 (1 H, m), 2.86–2.96 (1 H, m), 3.31 (1 H, dd, *J* 9.1 and 6.0), 3.57 (1 H, t, *J* 9.1), 3.81–3.90 (1 H, m), 4.00 (1 H, d, *J* 6.1), 4.61 (2 H, s), 7.26, 8.56 (4 H, AA′BB′, *J* 5.8), 7.33, 7.45 (4 H, AA′BB′, *J* 8.5); $\delta_C$(75 MHz; $CDCl_3$) 24.3, 26.3, 41.3, 47.7, 51.7, 55.3, 66.1, 68.9, 121.3, 123.4, 128.6, 131.6, 140.7, 143.6, 150.2, 176.2, 177.3; MALDI-HR-MS calcd for $C_{21}H_{21}BrN_3O_2^+$ ([M + H]$^+$): 426.0812; found: 426.0810.

### 4-[(3a*SR*,4*RS*,8a*SR*,8b*RS*)-2-(4-Methoxybenzyl)-1,3-dioxodecahydropyrrolo[3,4-*a*]pyrrolizin-4-yl]benzonitrile ((±)-20)

General procedure E, method B, starting from (±)-**16** (2.40 g, 5.25 mmol), [$Pd_2(dba)_3$] (300 mg, 0.32 mmol), dppf (350 mg, 0.63 mmol) and $Zn(CN)_2$ (622 mg, 5.25 mmol) in DMF (5 cm$^3$), gave (±)-**20** (1.66 g, 78%) as a colorless solid; mp 161–164 °C; $\nu_{max}$/cm$^{-1}$ (neat) 2958, 2833, 2224, 2051, 1979, 1767, 1703, 1683, 1652, 1608, 1584, 1514, 1463, 1432, 1393, 1341, 1318, 1299, 1250, 1202, 1169, 1111, 1086, 1036; $\delta_H$(300 MHz; $CDCl_3$) 1.57–1.87 (2 H, m), 1.95–2.20 (2 H, m), 2.54–2.64 (1 H, m), 2.80–2.91 (1 H, m), 3.28 (1 H, d, *J* 8.0), 3.49 (1 H, t, *J* 8.5), 3.73–3.81 (1 H, m), 3.79 (3 H, s), 4.08 (1 H, d, *J* 8.8), 4.39, 4.51 (2 H, AB, *J* 14.0), 6.80, 7.29 (4 H, AA′BB′, *J* 8.4), 7.21, 7.48 (4 H, AA′BB′, *J* 8.4); $\delta_C$(75 MHz; $CDCl_3$) 23.6, 29.8, 42.2, 49.3, 50.7; 51.1, 55.5, 68.2, 68.6, 111.6, 114.0, 119.2, 128.1, 129.0, 130.7, 132.1, 144.1, 159.5, 175.2, 177.9; MALDI-HR-MS calcd for $C_{24}H_{24}N_3O_3^+$ ([M + H]$^+$): 402.1812; found: 402.1817.

### 4-[(3a*SR*,4*RS*,8a*SR*,8b*RS*)-1,3-Dioxo-2-pyridin-4-ylmethyldecahydropyrrolo[3,4-*a*]pyrrolizin-4-yl]benzonitrile ((±)-21)

General procedure E, method A, starting from (±)-**17** (426 mg, 1.0 mmol) and CuCN (358 mg, 4.0 mmol) in DMF (4 cm$^3$), gave (±)-**21** (119 mg, 32%) as a colorless solid; mp (AcOEt) 200–202 °C; $\nu_{max}$/cm$^{-1}$ (neat) 3045, 2968, 2221, 1779, 1705, 1601, 1505, 1424, 1416, 1400, 1361, 1341, 1200, 1174; $\delta_H$(300 MHz; $CDCl_3$) 1.60–1.88 (2 H, m), 1.96–2.21 (2 H, m), 2.54–2.65 (1 H, m), 2.81–2.94 (1 H, m), 3.36 (1 H, d, *J* 7.8), 3.56 (1 H, dd, *J* 8.4 and 8.1), 3.77 (1 H, dd, *J* 9.9 and 6.9), 4.13 (1 H, d, *J* 8.4), 4.47, 4.53 (2 H, AB, *J* 14.7), 7.14, 8.53 (4 H, AA′BB′, *J* 5.7), 7.34, 7.51 (4 H, AA′BB′, *J* 8.4); $\delta_C$(75 MHz; $CDCl_3$) 23.6, 29.8, 41.5, 49.0, 50.8, 51.0, 68.3, 68.5, 111.8, 119.0, 123.4, 128.9, 132.2, 143.6, 144.2, 150.3, 174.9, 177.7; MALDI-HR-MS calcd for $C_{22}H_{21}N_4O_2^+$ ([M + H]$^+$): 373.1665; found: 373.1653.

### 4-[(3a*SR*,4*RS*,8a*SR*,8b*RS*)- and 4-[(3a*SR*,4*SR*,8a*RS*,8b*RS*)-2-(4-Bromobenzyl)-1,3-dioxodecahydropyrrolo[3,4-*a*]pyrrolizin-4-yl]benzonitrile ((±)-24 and (±)-25)

General procedure B, starting from **23** (1.0 g, 3.8 mmol), L-proline (459 mg, 4.0 mmol) and formylbenzonitrile (523 mg, 4.0 mmol) in $CH_3CN$ (20 cm$^3$), gave *endo*-adduct (±)-**24** (701 mg, 41%) and *exo*-adduct (±)-**25** (650 mg, 38%).

**Data for (±)-24.** Brown solid; mp 160–162 °C; $\nu_{max}$/cm$^{-1}$ (neat) 2959, 2886, 2842, 2223, 1771, 1702, 1607, 1489, 1429, 1393, 1333, 1299, 1166, 1087, 1071, 1014; $\delta_H$(300 MHz; $CDCl_3$) 1.59–1.85 (2 H, m), 1.96–2.18 (2 H, m), 2.54–2.63 (1 H, m), 2.81–2.91 (1 H, m), 3.30 (1 H, d, *J* 7.8), 3.52 (1 H, dd, *J* 8.4 and 8.1), 3.75 (1 H, dd, *J* 10.0 and 7.2), 4.10 (1 H, d, *J* 8.7), 4.41, 4.48 (2 H, AB, *J* 14.4), 7.14, 7.40 (4 H, AA′BB′, *J* 8.4), 7.29, 7.49 (4 H, AA′BB′, *J* 8.4); $\delta_C$(75 MHz; $CDCl_3$) 23.6, 29.8, 42.0, 49.2, 50.7, 51.0, 68.2, 68.6, 111.7, 119.1, 122.3, 129.0, 130.9, 131.9, 132.2, 134.8, 143.9, 175.1, 177.8; MALDI-HR-MS calcd for $C_{23}H_{21}BrN_3O_2^+$ ([M + H]$^+$): 450.0812; found: 450.0805.

**Data for (±)-25.** Brown solid; mp 116–119 °C; $\nu_{max}$/cm$^{-1}$ (neat) 2955, 2876, 2806, 2224, 1771, 1703, 1608, 1489, 1431, 1393, 1332, 1295, 1162, 1107, 1071, 1014; $\delta_H$(300 MHz; $CDCl_3$) 1.81–1.95 (2 H, m), 1.98–2.23 (3 H, m), 2.69–2.78 (1 H, m), 2.87–2.95 (1 H, m), 3.12–3.18 (1 H, m), 3.61–3.66 (2 H, m), 4.41, 4.54 (2 H, AB, *J* 14.0), 7.10, 7.44 (4 H, AA′BB′, *J* 8.4), 7.19, 7.47 (4 H, AA′BB′, *J* 8.4); $\delta_C$(75 MHz; $CDCl_3$) 22.7, 27.2, 41.8, 43.6, 45.8, 56.0, 66.3, 70.8, 111.5, 118.8, 122.0, 128.2, 130.7, 131.5, 131.9, 134.7, 142.4, 174.7, 175.3; MALDI-HR-MS calcd for $C_{23}H_{21}BrN_3O_2^+$ ([M + H]$^+$): 450.0812; found: 450.0805.

### 4-[(3a*SR*,4*RS*,8a*SR*,8b*RS*)-2-(4-Bromobenzyl)-1,3-dioxodecahydropyrrolo[3,4-*a*]pyrrolizin-4-yl]benzamidine hydrochloride ((±)-5)

General procedure F, starting from (±)-**24** (86 mg, 0.19 mmol), gave (±)-**5** (46 mg, 49%) as a colorless solid; mp 198–201 °C; $\nu_{max}$/cm$^{-1}$ (neat) 3411, 3328, 3253, 3158, 3050, 2960, 2871, 1771, 1683, 1651, 1610, 1535, 1489, 1435, 1415, 1398, 1347, 1299, 1282, 1170, 1094, 1078, 1043, 1016; $\delta_H$(300 MHz; $CD_3OD$) 1.60–1.78 (2 H, m), 1.89–2.06 (2 H, m), 2.43–2.55 (1 H, m), 2.69–2.81 (1 H, m), 3.45 (1 H, d, *J* 8.1), 3.54 (1 H, dd, *J* 8.1 and 7.8), 3.71 (1 H, dd, *J* 8.1 and 8.4), 4.16 (1 H, d, *J* 8.7), 4.36, 4.44 (2 H, AB, *J* 15.0), 7.12, 7.55 (4 H, AA′BB′, *J* 8.4), 7.27, 7.73 (4 H, AA′BB′, *J* 8.4); $\delta_C$(75 MHz; $CD_3OD$) 23.5, 29.7, 41.9, 48.6, 50.6, 51.0, 53.5, 68.0, 121.9, 126.2, 127.8, 129.0, 129.9, 131.7, 134.1, 145.2, 165.4, 176.2, 177.4; MALDI-HR-MS calcd for $C_{23}H_{24}BrN_4O_2^+$ ([M + H]$^+$): 468.1155; found: 468.1147.

### 4-[(3a*SR*,4*RS*,8a*SR*,8b*RS*)-2-(4-Methoxybenzyl)-1,3-dioxodecahydropyrrolo[3,4-*a*]pyrrolizin-4-yl]benzamidine hydrochloride ((±)-6)

General procedure F, starting from (±)-**20** (200 mg, 0.5 mmol), gave (±)-**6** (47 mg, 21%) as a colorless solid; mp 193–196 °C; $\nu_{max}$/cm$^{-1}$ (neat) 3421, 3264, 3065, 2966, 2873, 1771, 1694, 1613, 1538, 1516, 1484, 1462, 1438, 1404, 1348, 1300, 1256, 1210, 1175, 1095, 1029; $\delta_H$(300 MHz; $CDCl_3$) 1.57–1.73 (2 H, m), 1.82–1.95 (1 H, m), 2.00–2.12 (1 H, m), 2.29–2.41 (1 H, m), 2.58–2.70 (1 H, m), 3.25 (1 H, d, *J* 7.7), 3.54 (1 H, dd, *J* 8.0 and 7.7), 3.64 (1 H, dd, *J* 8.8 and 8.0), 3.71 (3 H, s), 4.09 (1 H, d, *J* 7.7), 4.30, 4.43 (2 H, AB, *J* 14.0), 6.73, 6.99 (4 H, AA′BB′, *J* 8.4), 7.47, 7.79 (4 H, AA′BB′, *J* 8.1), 8.74 (2H, bs); 9.16 (2H, bs); $\delta_C$(75 MHz; $CDCl_3$) 23.6, 29.9, 42.2, 48.8, 50.6, 51.1, 55.6, 68.3, 114.2, 126.9, 127.5, 128.3, 129.4, 130.0, 145.6, 159.5, 166.1, 176.8, 177.8; MALDI-HR-MS calcd for $C_{24}H_{27}N_4O_3^+$ ([M + H]$^+$): 419.2078; found: 419.2071.

### 4-[(3a*SR*,4*RS*,8a*SR*,8b*RS*)-1,3-Dioxo-2-pyridin-4-ylmethyldecahydropyrrolo[3,4-*a*]pyrrolizin-4-yl]benzamidine hydrochloride ((±)-7)

General procedure F, starting from (±)-**21** (87 mg, 0.23 mmol), gave (±)-**7** (27 mg, 28%) as a colorless solid; mp 204–207 °C;

 

$\nu_{max}$/cm$^{-1}$ (neat) 3322, 3204, 3059, 2972, 1772, 1695, 1675, 1608, 1561, 1538, 1484, 1419, 1399, 1338, 1317, 1174, 1082, 1048, 1017, 1008; $\delta_H$(300 MHz; $CD_3OD$) 1.76–1.93 (2 H, m), 2.05–2.19 (2 H, m), 2.62–2.71 (1 H, m), 2.88–2.97 (1 H, m), 3.53 (1 H, d, *J* 7.8), 3.75 (1 H, dd, *J* 9.0 and 7.8), 3.83 (1 H, t, *J* 8.4), 4.36 (1 H, d, *J* 8.4,), 4.54, 4.59 (2 H, AB, *J* 15.6), 7.29, 8.49 (4 H, AA′BB′, *J* 6.0), 7.54, 7.67 (4 H, AA′BB′, *J* 8.1); $\delta_C$(75 MHz; $CD_3OD$) 23.9, 30.2, 41.7, 49.9, 51.7, 51.8, 68.9, 69.3, 123.9, 128.0, 128.2, 129.8, 146.3, 147.0, 149.8, 167.7, 176.5, 179.3; MALDI-HR-MS calcd for $C_{22}H_{24}N_5O_2^+$ ([M + H]$^+$): 390.1925; found: 390.1920.

### 4-[(3a*SR*,4*RS*,8a*SR*,8b*RS*)-2-(4-Hydroxybenzyl)-1,3-dioxodecahydropyrrolo[3,4-*a*]pyrrolizin-4-yl]benzamidine hydrochloride ((±)-8)

A solution of methyl ether (±)-**20** (220 mg, 0.55 mmol) in dry $CH_2Cl_2$ (5 cm$^3$) under Ar was cooled to −50 °C, then $BBr_3$ (1.2 cm$^3$, 1.2 mmol, 1 M in $CH_2Cl_2$) was added and the mixture stirred for 8 h at 25 °C. The reaction mixture was poured onto ice and stirred for 30 min, before being extracted with $CH_2Cl_2$ (3 × 10 cm$^3$). The organic phase was dried ($Na_2SO_4$) and concentrated *in vacuo*. The residue showed decomposition upon purification by CC, therefore the crude product was used directly following general procedure F, giving (±)-**8** (31 mg, 40% over two steps) as a brown solid; mp 173–175 °C; $\nu_{max}$/cm$^{-1}$ (neat) 3344, 3204, 3122, 2961, 2873, 1771, 1674, 1612, 1538, 1515, 1486, 1431, 1398, 1339, 1287, 1232, 1204, 1171, 1090, 1045, 1018; $\delta_H$(300 MHz; $CD_3OD$) 1.72–1.86 (2 H, m), 2.00–2.15 (2 H, m), 2.57–2.66 (1 H, m), 2.77–2.87 (1 H, m), 3.40 (1 H, d, *J* 7.8), 3.38–3.73 (2 H, m), 4.20 (1 H, d, *J* 9.0), 4.37, 4.45 (2 H, AB, *J* 14.4), 6.71, 7.08 (4 H, AA′BB′, *J* 8.7), 7.25, 7.70 (4 H, AA′BB′, *J* 8.4); $\delta_C$(75 MHz; $CD_3OD$) 23.8, 30.0, 42.3, 49.9, 51.5, 69.1, 115.7, 116.6, 127.9, 128.1, 130.0, 130.57, 133.8, 146.5, 157.8, 167.9, 176.9, 179.7. In the $^{13}$C NMR spectrum of compound (±)-**8**, two resonances are buried under the solvent peak. MALDI-HR-MS calcd for $C_{23}H_{26}N_4O_3^+$ ([M + H]$^+$): 405.1921; found: 405.1917.

### 4-(3a*SR*,4*RS*,8a*SR*,8b*RS*)-(4-Bromophenyl)-2-(4-chlorobenzyl)-hexahydropyrrolo[3,4-*a*]-pyrrolizin-1,3-dione ((±)-26)

General procedure B, starting from **37** (see ESI†) (3.50 g, 15.8 mmol), L-proline (1.91 g, 16.6 mmol) and 4-bromobenzaldehyde (3.07 g, 16.6 mmol) in $CH_3CN$ (50 cm$^3$), gave *endo*-adduct (±)-**26** (3.34 g, 46%) as a colorless solid; mp 161–163 °C; $\nu_{max}$/cm$^{-1}$ (neat) 2963, 2873, 1698, 1695, 1486, 1423, 1393, 1337, 1168, 1089, 1069, 1042, 1006; $\delta_H$(300 MHz; $CDCl_3$) 1.57–1.85 (2 H, m), 1.95–2.17 (2 H, m), 2.57–2.61 (1 H, m), 2.77–2.89 (1 H, m), 3.27 (1 H, d, *J* 7.8), 3.46 (1 H, dd, *J* 8.3 and 8.1), 3.75 (1 H, dd, *J* 10.0 and 7.2), 4.01 (1 H, d, *J* 8.7), 4.48 (2 H, s), 7.06, 7.35 (4 H, AA′BB′, *J* 8.4), 7.20–7.29 (4 H, m); $\delta_C$(75 MHz; $CDCl_3$) 23.5, 29.7, 41.8, 49.1, 50.5, 50.8, 67.9, 68.2, 121.5, 128.6, 129.6, 130.3, 131.2, 133.7, 134.1, 136.9, 174.9, 177.6; MALDI-HR-MS calcd for $C_{22}H_{21}BrClN_2O_2^+$ ([M + H]$^+$): 459.0469; found: 459.0464.

### 4-(1*RS*,3a*SR*,4*RS*,8a*SR*,8b*RS*)-(4-Bromophenyl)-2-(4-chlorobenzyl)-1-(toluene-4-sulfonyl)octahydropyrrolo[3,4-*a*]pyrrolizin-3-one ((±)-30)

General procedure C, starting from (±)-**26** (3.30 g, 7.2 mmol), Li[$Et_3BH$] solution (13.7 cm$^3$, 13.7 mmol), 4-toluenesulfinic acid (3.04 g, 19.4 mmol) and $CaCl_2$ (2.15 g, 19.4 mmol) in $CH_2Cl_2$ (100 cm$^3$), gave (±)-**30** (1.55 g, 32%) as a colorless solid; mp 183–186 °C; $\nu_{max}$/cm$^{-1}$ (neat) 2982, 2940, 2877, 1711, 1595, 1488, 1386, 1292, 1199, 1136, 1083, 1007; $\delta_H$(300 MHz; $CDCl_3$) 1.52–1.72 (2 H, m), 1.85–2.04 (2 H, m), 2.42–2.50 (1 H, m), 2.47 (3 H, s), 2.52–2.58 (1 H, m), 2.81–2.88 (1 H, m), 2.95–2.98 (1 H, m), 3.02–3.08 (1 H, m), 3.90 (1 H, d, *J* 6.3), 4.14, 5.09 (2 H, AB, *J* 15.0), 4.26 (1 H, s), 7.15, 7.34 (4 H, AA′BB′, *J* 8.4), 7.18, 7.40 (4 H, AA′BB′, *J* 8.4), 7.39, 7.71 (4 H, AA′BB′, *J* 8.4); $\delta_C$(75 MHz; $CDCl_3$) 22.0, 24.6, 32.0, 43.1, 44.7, 51.1, 51.9, 69.7, 71.6, 81.3, 121.3, 125.4, 129.2, 129.6, 129.9, 130.0, 130.7, 131.1, 132.2, 134.0, 137.2, 146.5, 172.8; MALDI-HR-MS calcd for $C_{29}H_{29}BrClN_2O_3S^+$ ([M + H]$^+$): 599.0765; found 599.0755.

### 4-(1*RS*,3a*SR*,4*RS*,8a*SR*,8b*RS*)-(4-Bromophenyl)-2-(4-methoxybenzyl)-1-(toluene-4-sulfonyl)octahydropyrrolo[3,4-*a*]pyrrolizin-3-one ((±)-31)

General procedure C, starting from (±)-**16** (3.51 g, 7.70 mmol), Li[$Et_3BH$] solution (8.34 cm$^3$, 8.34 mmol), 4-toluenesulfinic acid (3.53 g, 20.8 mmol) and $CaCl_2$ (2.31 g, 20.8 mmol) in $CH_2Cl_2$ (100 cm$^3$), gave (±)-**31** (4.45 g, 97%) as a colorless solid; mp 206–207 °C; $\nu_{max}$/cm$^{-1}$ (neat) 2940, 2874, 1713, 1612, 1584, 1512, 1486, 1443, 1386, 1365, 1328, 1302, 1289, 1251, 1198, 1173, 1135, 1082, 1032, 1007; $\delta_H$(300 MHz; $CDCl_3$): 1.51–1.70 (2 H, m), 1.82–2.01 (2 H, m), 2.37–2.56 (2 H, m), 2.47 (3 H, s), 2.80–2.89 (1 H, m), 2.94 (1 H, dd, *J* 7.7 and 3.6), 2.99–3.05 (1 H, m), 3.82 (3 H, s), 3.89 (1 H, d, *J* 6.3), 4.00, 5.07 (2 H, AB, *J* 14.6), 4.27 (1 H, s), 6.88, 7.14 (4 H, AA′BB′, *J* 8.5), 7.16, 7.40 (4 H, AA′BB′, *J* 8.5), 7.39, 7.71 (4 H, AA′BB′, *J* 8.5); $\delta_C$(75 MHz; $CDCl_3$) 22.1, 24.8, 32.1, 43.3, 44.9, 51.4, 52.2, 55.5, 70.0, 71.4, 81.1, 114.4, 121.3, 127.3, 129.6, 129.9, 130.1, 130.7, 131.1, 132.5, 137.5, 146.4, 159.5, 172.7; MALDI-HR-MS calcd for $C_{30}H_{32}BrN_2O_4S^+$ ([M + H]$^+$): 595.1254; found: 595.1261.

### 4-(1*RS*,3a*SR*,4*RS*,8a*SR*,8b*RS*)-(4-Bromophenyl)-2-(4-chlorobenzyl)-1-isopropyloctahydropyrrolo[3,4-*a*]pyrrolizin-3-one ((±)-32)

General procedure D, starting from (±)-**30** (1.55 g, 2.58 mmol), $ZnCl_2$ solution (2.84 cm$^3$, 2.84 mmol) and Pr$^i$MgCl solution (2.58 cm$^3$, 5.16 mmol) in $CH_2Cl_2$ (50 cm$^3$), gave (±)-**32** (768 mg, 61%) as a yellowish solid; mp 195–198 °C; $\nu_{max}$/cm$^{-1}$ (neat) 2963, 2900, 2859, 2821, 2774, 1672, 1488, 1446, 1431, 1251, 1151, 1128, 1086, 1068, 1017, 1008; $\delta_H$(300 MHz; $CDCl_3$) 0.70 (3 H, d, *J* 6.8), 0.91 (3 H, d, *J* 6.8), 1.50–1.81 (2 H, m), 1.88–2.10 (3 H, m), 2.49 (1 H, dt, *J* 6.2 and 2.5), 2.56–2.67 (1 H, m), 2.85–2.98 (1 H, m), 3.18–3.27 (2 H, m), 3.30 (1 H, dd, *J* 8.4 and 8.1), 3.78, 4.82 (2 H, AB, *J* 14.9), 4.08 (1 H, d, *J* 7.5), 7.10, 7.44 (4 H, AA′BB′, *J* 8.4), 7.29 (4 H, d, *J* 8.4); $\delta_C$(75 MHz; $CDCl_3$) 14.9, 18.6, 24.7, 28.2, 31.5, 41.6, 43.5, 52.5, 52.9, 67.6, 70.2, 73.5, 121.0, 128.9, 129.6, 130.0, 131.1, 133.3, 135.4, 138.9, 172.8; MALDI-HR-MS calcd for $C_{25}H_{29}BrClN_2O^+$ ([M + H]$^+$): 487.1146; found: 487.1139.

### 4-(1*RS*,3a*SR*,4*RS*,8a*SR*,8b*RS*)-(4-Bromophenyl)-1-isopropyl-2-(4-methoxybenzyl)octahydropyrrolo[3,4-*a*]pyrrolizin-3-one ((±)-33)

General procedure D, starting from (±)-**31** (4.45 g, 7.47 mmol), $ZnCl_2$ solution (11.2 cm$^3$, 11.2 mmol) and Pr$^i$MgCl solution

(9.34 $cm^3$, 18.7 mmol) in $CH_2Cl_2$ (50 $cm^3$), gave (±)-**33** (1.64 g, 46%) as a brown solid; mp 72–75 °C; $\nu_{max}/cm^{-1}$ (neat) 2957, 1683, 1612, 1586, 1511, 1485, 1435, 1418, 1289, 1243, 1174, 1101, 1070, 1033, 1009; $\delta_H$(300 MHz; $CDCl_3$) 0.70 (3 H, d, *J* 6.9), 0.90 (3 H, d, *J* 6.9), 1.53–1.62 (1 H, m), 1.66–1.77 (1 H, m), 1.87–2.11 (3 H, m), 2.46 (1 H, dt, *J* 9.0 and 3.0), 2.56–2.65 (1 H, m), 2.88–2.96 (1 H, m), 3.16–3.26 (2 H, m), 3.30 (1 H, dd, *J* 8.4 and 7.8), 3.71, 4.82 (2 H, AB, *J* 14.8), 3.81 (3 H, s), 4.07 (1 H, d, *J* 7.8), 6.84, 7.28 (4 H, AA′BB′, *J* 8.4), 7.05, 7.43 (4 H, AA′BB′, *J* 8.4); $\delta_C$(75 MHz; $CDCl_3$) 14.8, 18.6, 24.6, 27.9, 31.4, 41.7, 43.4, 52.5, 52.9, 55.3, 67.1, 70.2, 73.1, 113.8, 120.6, 128.5, 129.3, 129.8, 130.7, 138.7, 158.7, 172.2; MALDI-HR-MS calcd for $C_{26}H_{32}BrN_2O_2^+$ ([M + H]$^+$): 483.1642; found: 483.1636.

### 4-[(1*RS*,3a*SR*,4*RS*,8a*SR*,8b*RS*)-2-(4-Chlorobenzyl)-1-isopropyl-3-oxodecahydropyrrolo[3,4-*a*]pyrrolizin-4-yl]benzonitrile ((±)-34)

General procedure E, method A, starting from (±)-**32** (570 mg, 1.17 mmol) and CuCN (419 mg, 4.7 mmol) in DMF (8 $cm^3$), gave (±)-**34** (217 mg, 43%) as a brown solid; mp 124–125 °C; $\nu_{max}/cm^{-1}$ (neat) 2963, 2900, 2823, 2229, 1671, 1608, 1490, 1447, 1434, 1412, 1390, 1349, 1266, 1251, 1126, 1087, 1017; $\delta_H$(300 MHz; $CDCl_3$) 0.69 (3 H, d, *J* 6.7), 0.90 (3 H, d, *J* 6.7), 1.50–1.68 (1 H, m), 1.65–1.81 (1 H, m), 1.87–2.09 (3 H, m), 2.50 (1 H, ddd, *J* 8.7, 2.8 and 2.5), 2.53–2.61 (1 H, m), 2.88–2.98 (1 H, m), 3.17–3.26 (2 H, m), 3.33 (1 H, dd, *J* 8.1 and 7.8), 3.79, 4.77 (2 H, AB, *J* 15.3), 4.15 (1 H, d, *J* 7.5), 7.11, 7.27 (4 H, AA′BB′, *J* 8.4,), 7.52, 7.58 (4 H, AA′BB′, *J* 8.4); $\delta_C$(75 MHz; $CDCl_3$) 15.0, 18.6, 24.8, 28.3, 31.5, 41.4, 43.4, 52.5, 53.0, 67.6, 70.4, 73.5, 110.4, 119.3, 128.6, 128.8, 129.3, 131.5, 133.1, 135.1, 145.7, 172.2; MALDI-HR-MS calcd for $C_{26}H_{29}ClN_3O^+$ ([M + H]$^+$): 434.1994; found: 434.1987.

### 4-[(1*RS*,3a*SR*,4*RS*,8a*SR*,8b*RS*)-1-Isopropyl-2-(4-methoxybenzyl)-3-oxodecahydropyrrolo[3,4-*a*]pyrrolizin-4-yl]benzonitrile ((±)-35)

General procedure E, method B, starting from (±)-**33** (351 mg, 0.73 mmol), [$Pd_2(dba)_3$] (41 mg, 0.04 mmol), dppf (49 mg, 0.09 mmol) and $Zn(CN)_2$ (86 mg, 0.73 mmol) in DMF (5 $cm^3$), gave (±)-**35** (205 mg, 62%) as a brown solid; mp 166–168 °C; $\nu_{max}/cm^{-1}$ (neat) 2960, 2873, 2224, 1684, 1610, 1584, 1512, 1437, 1414, 1390, 1367, 1339, 1300, 1245, 1175, 1101, 1036; $\delta_H$(300 MHz; $CDCl_3$) 0.70 (3 H, d, *J* 6.9), 0.90 (3 H, d, *J* 6.9), 1.52–1.60 (1 H, m), 1.66–1.77 (1 H, m), 1.90–2.14 (3 H, m), 2.47 (1 H, dt, *J* 9.0 and 2.7), 2.54–2.61 (1 H, m), 2.90–2.98 (1 H, m), 3.19–3.26 (2 H, m), 3.34 (1 H, t, *J* 8.4), 3.72, 4.80 (2 H, AB, *J* 15.0), 3.81 (3 H, s), 4.14 (1 H, d, *J* 7.8), 6.84, 7.08 (4 H, AA′BB′, *J* 8.7), 7.52, 7.59 (4 H, AA′BB′, *J* 8.4); $\delta_C$(75 MHz; $CDCl_3$) 14.9, 18.6, 24.8, 28.0, 31.5, 41.5, 43.4, 52.6, 53.1, 55.3, 67.1, 70.5, 73.3, 110.4, 113.8, 119.3, 128.3, 128.8, 129.2, 131.5, 145.7, 158.7, 171.9; MALDI-HR-MS calcd for $C_{27}H_{30}N_3O_2^+$ ([M − H]$^+$): 428.2339; found: 428.2333.

### 4-[(1*RS*,3a*SR*,4*RS*,8a*SR*,8b*RS*)-2-(4-Chlorobenzyl)-1-isopropyl-3-oxodecahydropyrrolo[3,4-*a*]pyrrolizin-4-yl]benzamidine hydrochloride ((±)-12)

General procedure F, starting from (±)-**34** (68 mg, 0.16 mmol), gave (±)-**12** (42 mg, 55%) as a colorless solid; mp 200–203 °C; $\nu_{max}/cm^{-1}$ (neat) 3251, 3061, 2959, 2868, 1659, 1613, 1539, 1489, 1445, 1407, 1390, 1289, 1245, 1090, 1015; $\delta_H$(300 MHz; $CD_3OD$) 0.74 (3 H, d, *J* 6.8), 0.97 (3 H, d, *J* 6.8), 1.67–1.83 (2 H, m), 1.97–2.10 (2 H, m), 2.11–2.22 (1 H, m), 2.57–2.73 (2 H, m), 2.90–3.02 (1 H, m), 3.26–3.37 (2 H, m), 3.48 (1 H, dd, *J* 8.1 and 7.8), 3.97, 4.69 (2 H, AB, *J* 15.3), 4.33 (1 H, d, *J* 7.5), 7.27, 7.36 (4 H, AA′BB′, *J* 8.4), 7.62, 7.72 (4 H, AA′BB′, *J* 8.4); $\delta_C$(75 MHz; $CD_3OD$) 14.8, 18.4, 25.1, 29.1, 31.7, 42.0, 44.0, 53.1, 54.3, 69.3, 71.1, 74.8, 127.4, 127.9, 129.3, 129.9, 130.3, 134.0, 136.1, 147.7, 164.3, 167.8, 174.3; MALDI-HR-MS calcd for $C_{26}H_{32}ClN_4O^+$ ([M + H]$^+$): 451.2259; found: 451.2261.

### 4-[(1*RS*,3a*SR*,4*RS*,8a*SR*,8b*RS*)-1-Isopropyl-2-(4-methoxybenzyl)-3-oxodecahydropyrrolo[3,4-*a*]pyrrolizin-4-yl]benzamidine hydrochloride ((±)-13)

General procedure F, starting from (±)-**35** (205 mg, 0.45 mmol), gave (±)-**13** (54 mg, 25%) as a colorless solid; mp 215–218 °C; $\nu_{max}/cm^{-1}$ (neat) 3355, 2958, 2833, 2224, 1767, 1703, 1699, 1694, 1666, 1611, 1584, 1513, 1452, 1432, 1393, 1341, 1300, 1253, 1202, 1172, 1111, 1086, 1035; $\delta_H$(300 MHz; $(CD_3)_2SO$) 0.64 (3 H, d, *J* 6.5), 0.87 (3 H, d, *J* 6.9), 1.53–1.97 (2 H, m), 1.83–1.97 (2 H, m), 2.03–2.13 (1 H, m), 2.38–2.60 (2 H, m), 2.74–2.86 (1 H, m), 3.09–3.17 (2 H, m), 3.20–3.28 (1 H, m), 3.64, 4.55 (2 H, AB, *J* 14.8), 4.17 (1 H, d, *J* 7.2), 6.90, 7.12 (4 H, AA′BB′, *J* 8.4), 7.55, 7.75 (4 H, AA′BB′, *J* 7.8), 8.99 (2 H, bs), 9.31 (2 H, bs); $\delta_C$(75 MHz; $CD_3OD$) 15.3, 18.7, 25.3, 28.5, 31.9, 41.4, 51.0, 52.2, 53.9, 55.5, 67.9, 70.6, 73.7, 114.4, 126.1, 128.2, 128.4, 128.6, 129.4, 146.9, 159.3, 166.0, 172.6; MALDI-HR-MS calcd for $C_{27}H_{35}N_4O_2^+$ ([M + H]$^+$): 447.2755; found: 447.2749.

### X-Ray crystal structure of (±)-29

Crystal data at 173(2) K for $C_{22}H_{22}BrFN_2O_2$: $M_r$ = 445.33, triclinic, space group $P\bar{1}$ (no. 2), $D_c$ = 1.550 g $cm^{-3}$, $Z$ = 2, $a$ = 9.4567(2) Å, $b$ = 10.5163(2) Å, $c$ = 10.6619(2) Å, $\alpha$ = 78.900(1)°, $\beta$ = 89.899(1)°, $\gamma$ = 66.981(1)°, $V$ = 954.45(3) $Å^3$. Bruker–Nonius Kappa-CCD diffractometer, MoKα radiation, $\lambda$ = 0.7107 Å, $\mu$ = 2.184 $mm^{-1}$. Crystal dimensions *ca.* 0.18 × 0.16 × 0.15 mm. The numbers of measured and unique reflections were 7417 and 4368, respectively ($R_{int}$ = 0.016). The structure was solved by direct methods (SIR-97)[21] and refined by full-matrix least-squares analysis (SHELXL-97),[22] using an isotropic extinction correction. All non H-atoms were refined anisotropically, H-atoms isotropically, whereby H-positions are based on stereochemical considerations. Final $R(F)$ = 0.029, $wR(F^2)$ = 0.064 for 276 parameters and 3942 reflections with $I > 2\sigma(I)$ and 3.76 < $\theta$ < 27.50° (corresponding $R$ values based on all 4368 reflections are 0.034 and 0.067 respectively).

Crystallographic data (excluding structure factors) for the structure reported in this paper have been deposited with the Cambridge Crystallographic Data Centre: CCDC reference number 297366. For crystallographic data in CIF or other electronic format see DOI: 10.1039/b602585d

### X-Ray crystal structure of the complex of thrombin with (+)-13

Diffraction data were measured on a Bruker FR591 X-ray generator, with 0.2 mm focus, run at 50 kV/60 mA and equipped with an Osmic focussing monochromator and an Oxford Cryostream cooler run at 100 K. The Marresearch300 image plate detector

 

was placed 120 mm from the crystal and scanned with 0.15 mm pixel size. Exposure times were 600 s for 0.5° frames. Data from 456 frames were processed to 1.79 Å resolution using XDS.[23] The space group is $C2$ with unit cell dimensions $a = 71.29$ Å, $b = 71.84$ Å, $c = 73.06$ Å, $\beta = 100.56°$. For 141 897 observations of 31 281 reflections (with ice rings excluded 2.28–2.22 Å and 1.92–1.89 Å), the merging $R$ factor on intensities was 4.1% (25.3% in the outermost shell, 1.79–1.9 Å), with completeness 91.4% (86.6%) and $I/\sigma$ 22.9 (5.4). Data reduction used the CCP4 package.[24] Starting from 1OYT.pdb, model building with MOLOC[19] and refinement with Refmac5[25] to 1.79 Å resolution gave for 29 702 (working) and 1582 (free) reflections, final overall crystallographic $R$ factors of 16.0% and 19.8%, with values in the outer shell (1.83–1.79 Å) of 20.5% and 24.8%, respectively, for 2827 non-hydrogen atoms, including one $Na^+$ ion, one $Ca^{2+}$ ion and 493 water molecules. The inhibitor density is very clear. Coordinates have been deposited at the Protein Data Bank, PDB code: 2CF9.

#### X-Ray crystal structure of the complex of thrombin with (+)-12

Diffraction data were measured at the Swiss Light Source (SLS) on beamline PXII. The wavelength was 0.97001 Å, the detector MarCCD225 at 120 mm, and exposure times were 1 s for 360 frames of 0.5°. The images showed no ice rings and ~10 overloads per image. The data were processed to 1.3 Å resolution using XDS, including the 'zero dose' radiation damage correction with default values. The space group is $C2$ with unit cell dimensions $a = 71.07$ Å, $b = 71.51$ Å, $c = 72.40$ Å, $\beta = 100.25°$. For 307621 observations of 85919 reflections, the merging $R$ factor on intensities was 3.9% (30.2% in the outermost shell, 1.37–1.3 Å), with completeness 98.2% (95.9%) and $I/\sigma$ 17.8 (4.2). Data reduction was as above. Refinement with Refmac5 used the TLS option and hydrogens were inserted at riding positions, where unique. The final overall crystallographic $R$ factors are 18.0% (working) and 19.9% (free), with values in the outer shell (1.334–1.30 Å) of 26.3% and 29.6%, respectively, for 81 614 (4308) reflections and 2789 non-hydrogen atoms, including one $Na^+$ ion, one $Ca^{2+}$ ion and 397 water molecules. Seven residues were given alternative conformations. The inhibitor density is very clear. Coordinates have been deposited at the Protein Data Bank, PDB code: 2CF8.

## Acknowledgements

Support from F. Hoffmann–La Roche Ltd, Chugai Pharmaceuticals and the ETH Research Council is gratefully acknowledged. We thank Olivier Kuster for the measurement of enzyme inhibitor constants and Andri Schütz and Tobias Platen for their help in the preparation of some compounds. This work was further supported by postdoctoral fellowships to A. H.-R. (Emmy Noether-Program, DFG) and J. A. O. (Carlsberg Foundation).

## References

1 (*a*) U. Obst, V. Gramlich, F. Diederich, L. Weber and D. W. Banner, *Angew. Chem., Int. Ed. Engl.*, 1995, **34**, 1739–1742; (*b*) U. Obst, D. W. Banner, L. Weber and F. Diederich, *Chem. Biol.*, 1997, **4**, 287–295.
2 (*a*) J. A. Olsen, D. W. Banner, P. Seiler, U. Obst Sander, A. D'Arcy, M. Stihle, K. Müller and F. Diederich, *Angew. Chem., Int. Ed.*, 2003, **42**, 2507–2511; (*b*) J. A. Olsen, D. W. Banner, P. Seiler, B. Wagner, T. Tschopp, U. Obst-Sander, M. Kansy, K. Müller and F. Diederich, *ChemBioChem*, 2004, **5**, 666–675; (*c*) J. Olsen, P. Seiler, B. Wagner, H. Fischer, T. Tschopp, U. Obst-Sander, D. W. Banner, M. Kansy, K. Müller and F. Diederich, *Org. Biomol. Chem.*, 2004, **2**, 1339–1352; (*d*) E. Schweizer, A. Hoffmann-Röder, K. Schärer, J. Olsen, C. Fäh, P. Seiler, U. Obst-Sander, B. Wagner, M. Kansy and F. Diederich, *ChemMedChem*, 2006, DOI: 10.1002/cmdc.200600015.
3 For a similar approach, see: (*a*) C.-Y. Kim, J. S. Chang, J. B. Doyon, T. T. Baird, Jr., C. A. Fierke, A. Jain and D. W. Christianson, *J. Am. Chem. Soc.*, 2000, **122**, 12125–12134; (*b*) R. D. Madder, C.-Y. Kim, P. P. Chandra, J. B. Doyon, T. A. Baird, Jr., C. A. Fierke, D. W. Christianson, J. G. Voet and A. Jain, *J. Org. Chem.*, 2002, **67**, 582–584.
4 For thrombin inhibitors, see: (*a*) J. B. M. Renwinkel and A. E. P. Adang, *Curr. Pharm. Des.*, 1999, **5**, 1043–1075; (*b*) J. A. Huntington and T. P. Baglin, *Trends Pharmacol. Sci.*, 2003, **24**, 589–595; (*c*) S. Srivastava, L. N. Goswami and D. K. Dikshit, *Med. Res. Rev.*, 2005, **25**, 66–92; (*d*) M. Di Nisio, S. Middeldorp and H. R. Büller, *New Engl. J. Med.*, 2005, **353**, 1028–1040.
5 F. Hof, D. M. Scofield, W. B. Schweizer and F. Diederich, *Angew. Chem., Int. Ed.*, 2004, **43**, 5056–5059.
6 R. Paulini, K. Müller and F. Diederich, *Angew. Chem., Int. Ed.*, 2005, **44**, 1788–1805.
7 U. Obst, P. Betschmann, C. Lerner, P. Seiler, F. Diederich, V. Gramlich, L. Weber, D. W. Banner and P. Schönholzer, *Helv. Chim. Acta*, 2000, **83**, 855–909.
8 (*a*) T. F. Braish and D. E. Fox, *Synlett*, 1992, 979–980; (*b*) C. J. Walter, H. L. Anderson and J. K. M. Sanders, *J. Chem. Soc., Chem. Commun.*, 1993, 458–460.
9 (*a*) R. Huisgen, *J. Org. Chem.*, 1976, **41**, 403–419; (*b*) R. Grigg, J. Idle, P. McMeekin and D. Vipond, *J. Chem. Soc., Chem. Commun.*, 1987, 49–51; (*c*) O. Tsuge and S. Kanemasa, *Adv. Heterocycl. Chem.*, 1989, **45**, 231–349.
10 (*a*) A. Pinner and F. Klein, *Ber. Dtsch. Chem. Ges.*, 1877, **10**, 1889–1897; (*b*) G. Wagner and I. Wunderlich, *Pharmazie*, 1977, **32**, 76–79.
11 J. F. W. McOmie, M. L. Watts and D. E. West, *Tetrahedron*, 1968, **24**, 2289–2292.
12 H. Bienaymé, *Angew. Chem., Int. Ed. Engl.*, 1997, **36**, 2670–2673.
13 A. Hoffmann-Röder, P. Seiler and F. Diederich, *Org. Biomol. Chem.*, 2004, **2**, 2267–2269.
14 D. S. Brown, P. Charreau, T. Hansson and S. V. Ley, *Tetrahedron*, 1991, **47**, 1311–1328.
15 (*a*) R. Lottenberg, J. A. Hall, M. Blinder, E. P. Binder and C. M. Jackson, *Biochim. Biophys. Acta*, 1983, **742**, 539–557; (*b*) J. W. Fenton, II, M. J. Fasco, A. B. Stackrow, D. L. Aronson, A. M. Young and J. S. Finlayson, *J. Biol. Chem.*, 1977, **252**, 3587–3598; (*c*) K. Hilpert, J. Ackermann, D. W. Banner, A. Gast, K. Gubernator, P. Hadváry, L. Labler, K. Müller, G. Schmid, T. B. Tschopp and H. van de Waterbeemd, *J. Med. Chem.*, 1994, **37**, 3889–3901.
16 P. Betschmann, S. Sahli, F. Diederich, U. Obst and V. Gramlich, *Helv. Chim. Acta*, 2002, **85**, 1210–1245.
17 K. Schärer, M. Morgenthaler, P. Seiler, F. Diederich, D. W. Banner, T. Tschopp and U. Obst-Sander, *Helv. Chim. Acta*, 2004, **87**, 2517–2538.
18 (*a*) W. Bode, I. Mayr, U. Baumann, R. Huber, S. R. Stone and J. Hofsteenge, *EMBO J.*, 1989, **8**, 3467–3475; (*b*) D. W. Banner and P. Hadváry, *J. Biol. Chem.*, 1991, **266**, 20085–20093; (*c*) W. Bode, D. Turk and A. Karshikov, *Protein Sci.*, 1992, **1**, 426–471.
19 P. R. Gerber and K. Müller, *J. Comput. Aided Mol. Des.*, 1995, **9**, 251–268; Gerber Molecular Design (http://www.moloc.ch).
20 L. F. Tietze and T. Eicher, *Reaktionen und Synthesen im Organisch-Chemischen Praktikum*, Thieme, Stuttgart, 1991, pp. 73–74.
21 A. Altomare, M. C. Burla, M. Camalli, G. L. Cascarano, C. Giacovazzo, A. Guagliardi, A. G. G. Moliterni, G. Polidori and R. Spagna, *J. Appl. Crystallogr.*, 1999, **32**, 115–119.
22 G. M. Sheldrick, *SHELXL-97, Program for refinement of crystal structures*, University of Göttingen, Germany, 1997.
23 W. Kabsch, *J. Appl. Crystallogr.*, 1993, **26**, 795–800.
24 Collaborative Computational Project, Number 4, *Acta Crystallogr., Sect. D: Biol. Crystallogr.*, 1994, **50**, 760–763.
25 G. N. Murshudov, A. A. Vagin and E. J. Dodson, *Acta Crystallogr., Sect. D: Biol. Crystallogr.*, 1997, **53**, 240–255.